Biochimica et Biophysica Acta 1820 (2012) 1859–1866

Contents lists available at SciVerse ScienceDirect

Biochimica et Biophysica Acta

journal homepage: www.elsevier.com/locate/bbagen

Entamoeba histolytica thioredoxin reductase: Molecular and functional characterization of its atypical properties

Diego G. Arias, Erika L. Regner, Alberto A. Iglesias, Sergio A. Guerrero *

Instituto de Agrobiotecnología del Litoral (UNL–CONICET), Facultad de Bioquímica y Ciencias Biológicas, Paraje "El Pozo" CC 242, S3000ZAA Santa Fe, Argentina

ARTICLE INFO

Article history:
Received 19 June 2012
Received in revised form 5 August 2012
Accepted 27 August 2012
Available online 3 September 2012

Keywords:
Entamoeba
Thioredoxin
S-nitrosothiol
Antioxidant
Reducing power

ABSTRACT

Background: Entamoeba histolytica, an intestinal protozoan that is the causative agent of amoebiasis, is exposed to elevated amounts of highly toxic reactive oxygen and nitrogen species during tissue invasion. Thioredoxin reductase catalyzes the reversible transfer of reducing equivalents between NADPH and thioredoxin, a small protein that plays key metabolic functions in maintaining the intracellular redox balance.
Methods: The present work deals with *in vitro* steady state kinetic studies aimed to reach a better understanding of the kinetic and structural properties of thioredoxin reductase from *E. histolytica* (*Eh*TRXR).
Results: Our results support that native *Eh*TRXR is a homodimeric covalent protein that is able to catalyze the NAD(P)H-dependent reduction of amoebic thioredoxins and *S*-nitrosothiols. In addition, the enzyme exhibited NAD(P)H dependent oxidase activity, which generates hydrogen peroxide from molecular oxygen. The enzyme can reduce compounds like methylene blue, quinones, ferricyanide or nitro-derivatives; all alternative substrates displaying a relative high capacity to inhibit disulfide reductase activity of *Eh*TRXR.
Conclusions and general significance: Interestingly, *Eh*TRXR exhibited kinetic and structural properties that differ from other low molecular weight TRXR. The TRX system could play an important role in the parasite defense against reactive species. The latter should be critical during the extra intestinal phase of the amoebic infection. So far we know, this is the first in depth characterization of *Eh*TRXR activity and functionality.

1. Introduction

Amoebiasis is an intestinal infection widespread throughout the world, caused by the human pathogen *Entamoeba histolytica* [CDC, http://www.cdc.gov/]. The parasitic disease is the third leading cause of death in almost all countries where sewage and water quality are inadequate, causing 50 million clinical episodes of dysentery or amoebic liver abscess and ca. 100,000 deaths annually [WHO, http://www.who.int/en/]. Identification and functional characterization of molecular targets are relevant matters for the rational design of new therapeutic drugs, which could improve the treatment of the disease. In this regard, processes involved in redox metabolism are of particular interest in *E. histolytica* [1,2]. It is known that the trofozoites of *E. histolytica* find in the anaerobic environment of the human gut a suitable place to live and multiply. However, during tissue invasion the microorganism is exposed to environments containing high levels of oxidizing reactive oxygen species (ROS) and reactive nitrogen species (RNS), such as nitric oxide (NO) [3,4]. NO can diffuse into *E. histolytica* cells and react with species derived from cysteine (the major intracellular low molecular mass thiol [5]) to perform CySNO. This metabolite is thought to be critical for *S*-nitrosylation (addition of NO to cysteine residue's thiol group) or *S*-thiolation (addition of cysteine to cysteine residue's thiol group) of cellular proteins [6].

It has been proposed that exposure to high concentrations of NO or *S*-nitrosothiols render an imbalance in redox potential leading to *E. histolytica* growth inhibition. *In vitro* studies demonstrated the inhibitory effect of GSNO on the activity of cysteine proteases and alcohol dehydrogenase 2, enzymes considered as important virulence factor for the cytopathogenecity and survival of this parasite, respectively [7]. Although NO and *S*-nitrosothiols are toxic *in vitro*, the pathogen can still survive and multiply during tissue invasion, this suggests that *E. histolytica* possesses a detoxification system to cope with these toxic agents. All living forms have developed efficient enzymatic systems to resist damage generated by ROS and RNS. The redox cellular status is a crucial mediator for different metabolic processes acting in signaling and regulation of several metabolic and cellular processes [8].

The thioredoxin system plays an important role as an antioxidant mechanism. It can take part in: i) regulation of enzymatic activities, ii) repairing oxidized proteins, iii) affording reducing equivalents for

Abbreviations: TRXR, thioredoxin reductase; TRX, thioredoxin; GSNO, *S*-nitrosoglutathione; CySNO, *S*-nitrosocysteine; MBQ, 2-methyl-benzoquinone; DTBBQ, 2-5-ditert-buthyl-benzoquinone; DTNB, 5-5′-dithio-nitrobenzoic acid; MB, methylene blue; MV, methyl viologen; CDNB, 1-chloro-2,4-dinitrobenzene

* Corresponding author at: Laboratorio de Bioquímica Microbiana, Instituto de Agrobiotecnología del Litoral (CONICET), Facultad de Bioquímica y Ciencias Biológicas, Universidad Nacional del Litoral (UNL), Santa Fe, (3000), Argentina. Tel.: +54 342 4575221 int. 131.
E-mail address: sguerrer@fbcb.unl.edu.ar (S.A. Guerrero).

0304-4165/$ – see front matter © 2012 Elsevier B.V. All rights reserved.
http://dx.doi.org/10.1016/j.bbagen.2012.08.020

DNA synthesis; as well as cellular transcription, growth and apoptosis [9,10]. We have reported the functional characterization and immunolocalization of a thioredoxin system from *E. histolytica* [11,12]. After these findings the metabolic redox scenario operative in *E. histolytica* was revisited, proposing a central and critical role of the thioredoxin system. The redox metabolism in the parasite is complemented with other components such as *Eh*2CysPrx (or *Eh*p29), Fe-superoxide dismutase (Fe-SOD), rubrerythrin, cysteine, flavoprotein A, and a 34 kDa oxidoreductase (*Eh*p34) [11].

In this work, we present new kinetic, structural and thermodynamic properties exhibited by *Eh*TRXR. We characterized the NAD(P)H-dependent reduction of 5,5′-dithiobis-(2-nitrobenzoic) acid, TRXs and *S*-nitrosothiols (such as GSNO and CySNO), gathering information that reinforces the right assignment structure-function for *Eh*TRXR and broads the functional relationship between the enzyme and the capacity of *E. histolytica* for coping with environmental oxidative conditions.

2. Materials and methods

2.1. Materials

Bacteriological media components were from Britania Laboratories (Rosario, Argentina). All other reagents and chemicals were of the highest quality commercially available.

2.2. Expression and purification

The pGEM-T Easy/*Eh*TRXR plasmid [11,12] and the pET28-a vector (Novagen) were digested with *Bam*HI and *Hind*III. Ligation to the pET28-a vector of the insert was performed using T4 DNA ligase for 16 h at 16 °C to generate the pET28/*Eh*TRXR plasmid. Preparation of plasmid DNA and subsequent restriction treatment were performed to check the correctness of the different constructs.

*Eh*TRXR, *Eh*TRX8 and *Eh*TRX41 were expressed in *Escherichia coli* BL21 (DE3) as His-tag (N-terminal) recombinant proteins, and they were chromatographically purified as previously described [11,12].

2.3. Protein methods

SDS-PAGE was carry out using the Bio-Rad minigel equipment, basically according to previously described methods [13,14]. Protein concentrations were determined by the method of Bradford [15], utilizing BSA as standard.

2.4. Determination of the molecular mass by gel filtration chromatography

The determination of the native molecular mass of proteins was performed by gel filtration chromatography in a Superdex 200 HR Tricorn column (GE). The calibration curve was constructed using the logarithm of the molecular masses (log MM) vs. the distribution coefficients (K_{av}) measured for each molecular mass standard: Thyroglobulin (669 kDa), Ferritin (440 kDa), Aldolase (158 kDa), Conalbumin (75 kDa), Ovalbumin (43 kDa), Carbonic anhydrase (29 kDa), Ribonuclease A (13.7 kDa) and Aprotinin (6.5 kDa) (Gel Filtration Calibration Kit-GE).

2.5. Preparation of S-nitrosothiols

GSNO or CySNO were prepared as previously described [16] by nitrosation under acid conditions. Briefly, equal volumes of glutathione or cysteine (both 200 mM) and sodium nitrite (200 mM) were incubated in the presence of 10 mM HCl on ice for 30 min. GSNO or CySNO were stabilized by addition of 1 mM EDTA at pH 7.0. GSNO or CySNO were freshly prepared and stored on ice in the dark. The concentration of GSNO and CySNO was estimated by measuring absorbance at 332 nm, using molar absorption coefficients of 0.92 mM^{-1} cm^{-1} and 0.75 mM^{-1} cm^{-1}, respectively [16].

2.6. EhTRXR assay and kinetic analysis

All enzymatic assays were performed spectrophotometrically at 30 °C using a Multiskan Ascent one-channel vertical light path filter photometer (Thermo Electron Co.). The general assay medium (GAM) contained 50 mM potassium phosphate, pH 7.0, and 2 mM EDTA, over which specific additions were made for each of the enzymes. In all the cases the final volume was of 50 μl.

TRXR activity was measured by monitoring NADPH oxidation at 340 nm with the addition to the GAM of 0.3 mM NADPH, 0.13 mM bovine insulin, 0.15–30 μM TRXs, and 0.1–1 μM *Eh*TRXR.

Activity for 5,5′-Dithiobis(2-nitrobenzoic acid) (DTNB) reductase was measured by monitoring the production of thionitrobenzoate at 405 nm after complementing the GAM with 0.3 mM NADPH, 0.078–10 mM DTNB, and 0.1–1 μM *Eh*TRXR. Activity was calculated using the molar extinction coefficient at 405 nm of 13.8 mM^{-1} cm^{-1} and considering that 1 mol of NADPH yields 2 mol of thionitrobenzoate [17].

Quinone reductase activity was measured by monitoring the oxidation of NADPH at 340 nm in a reaction mixture comprising GAM supplemented with 0.3 mM NADPH, 2–500 μM 2-methyl-benzoquinone or 2′-5′-di-tert-buthyl-benzoquinone, and 0.1–1 μM *Eh*TRXR.

Diaforase activity was measured by monitoring the oxidation of NADPH at 340 nm by addition to the GAM of 0.3 mM NADPH, 2–1000 μM ferricyanide or methylene blue, and 0.1–1 μM *Eh*TRXR.

Nitroreductase activity was measured by monitoring the oxidation of NADPH at 340 nm by supplementing GAM with 0.3 mM NADPH, 10–1000 μM 1-chloro-2,4-dinitrobenzene or methylviologen, and 0.1–1 μM *Eh*TRXR.

Hydrogen peroxide production due to NAD(P)H oxidase activity of the enzyme was determinate with the ferrithiocyanate method [18].

All kinetic data were plotted as initial velocity ($\mu M \cdot min^{-1}$) versus substrate concentration. The kinetic parameters were acquired by fitting the data with a nonlinear least-squares formula and the Michaelis–Menten equation using the program Origin. Kinetic constants are the mean of at least three independent sets of data, and they are reproducible within ±10%. In the study of inhibitors, IC_{50} refers to the concentration of the inhibitor giving 50% of the initial activity.

2.7. Determination of macroscopic redox potential of EhTRXR

The redox potential of *Eh*TRXR was determined by steady-state kinetics as described elsewhere [19,20]. All measurements were carried out in 50 mM potassium phosphate, pH 7.0, 2 mM EDTA at 30 °C. When *Ec*TRX_{Ox} (0.3–30 μM) was the electron acceptor, reaction rates were monitored by the decrease in absorbance at 340 nm due to oxidation of NADPH (1.5–300 μM) at 340 nm. In the reverse direction, where $NADP^+$ (7–1000 μM) was the electron acceptor, the increase in absorbance at 340 nm due to reduction of $NADP^+$ in the presence de of *Ec*TRX_{Red} (0.3–30 μM) was monitored. A constant level of *Ec*TRX_{Red} was maintained including 5 mM DTT in the buffer. Direct reductions of $NADP^+$ by *Eh*TRXR in presence of 5 mM DTT but without *Ec*TRX_{Red} were recorded for background correction. The steady-state kinetic parameter $k_{cat} \cdot K_m^{-1}$ represents the apparent second-order rate constant of the substrate-free enzyme reaction. Using Haldane equation, the equilibrium constants can be calculated, and the redox potential of the enzyme is then obtained from the Nernst equation [21]. A value of −320 mV and −283 mV were used as standard redox potential of $NADP^+$/NADPH and *Ec*TRX_{Ox}/*Ec*TRX_{Red} couples, respectively [19,20].

2.8. Stress resistance assays

For disk inhibition assays recombinant *E. coli* cells were grown overnight at 37 °C in LB broth containing kanamycin (50 $\mu g \cdot ml^{-1}$), then diluted 1/100 in LB medium and further incubated at 37 °C until a final optical density of 0.5. These cells were grown in the presence of 0.1 mM IPTG for another 4 h and then poured into plates with addition of IPTG and kanamycin. A sterilized filter disk (6 mm in diameter), previously soaked with 10 μl of either 20 or 200 mM diamide was placed in the middle of the plate. The plates were overnight incubated at 37 °C.

3. Results

3.1. EhTRXR is a FAD-containing covalent homodimer protein

Recombinant *Eh*TRXR exhibited an absorption spectrum with a pattern typical of a flavin-containing protein (Fig. 1), characterized by two peaks of maximal absorption at 380 and 453 nm. Under aerobic conditions, the peak at 453 nm decreased after addition of 100 μM NADPH (Fig. 1), indicating the reduction of the flavin prosthetic group. After that, the absorption at 453 nm began to increase towards initial values, which suggests an enzyme autooxidation in the presence of O_2 (Fig. 1). Denaturing *Eh*TRXR by boiling resulted in the flavin release, indicating a non-covalent association with the protein. The absorbance spectra of free flavin fraction (in comparison with spectrum of FAD or FMN standard) indicate that FAD rather than FMN forms the prosthetic group in *Eh*TRXR. For the purified enzyme we calculated that ~1 mol FAD is bound per mol of *Eh*TRXR subunit.

We observed that *Eh*TRXR modified their electrophoretic profile in nonreducing SDS-PAGE after incubation in the presence or the absence of 10 mM DTT. The "oxidized" enzyme showed a lower electrophoretic migration when compared with that incubated with DTT, migrating as a band of molecular mass ~64 kDa (Fig. 2). No profile modification was observed when the enzyme was incubated with its specific reducing substrate, NADPH (200 μM) or NADPH (200 μM) + DTNB (5 mM) (Fig. 2), indicating that the catalytic cysteine residues (active site) would not be forming the intracatenary disulfide bridge in the enzyme. No effect of diamide (10 mM) on the migration profile of *Eh*TRXR was observed. The behavior of the "oxidized" enzyme seems indicate the formation of an intercatenary disulfide bridge. On the other hand, the purified *Eh*TRXR eluted as a protein of 78 kDa in gel filtration chromatography (Fig. 3), thus revealing that the enzyme forms a homodimeric structure in its native active state, which is in agreement with sizes determined for native low molecular mass TRXR from other sources [22].

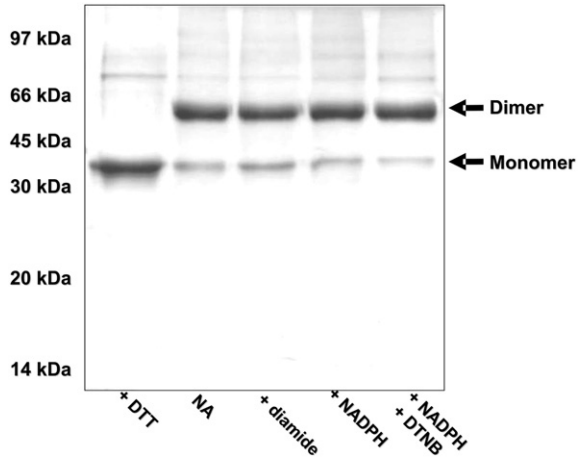

Fig. 2. Non-reducing SDS-PAGE of EhTRXR incubated in different conditions. The protein was incubated with: 100 mM DTT, no addition (NA), 10 mM diamide, 200 μM NADPH, or 200 μM NADPH + 5 mM DTNB. All incubations were performed for 10 min at 37 °C and pH 7.0.

3.2. EhTRXR can use NADPH or NADH as reducing substrate

Unlike to other TRXRs, *Eh*TRXR was able to use NADH as reducing equivalent donor (in the μM concentration range). This was evaluated by means of the NAD(P)H-dependent reduction of DTNB by *Eh*TRXR (Fig. 4). Steady state kinetic assays demonstrated that the reaction of DTNB reduction catalyzed by *Eh*TRXR with NADPH or NADH follows a "hybrid ping-pong" mechanism (data no shown); the latter being common for this type of enzymes [23]. Table 1 shows the kinetic parameters for DTNB-dependent oxidation of NADPH and NADH by *Eh*TRXR. Although the affinity exhibited by the entamoebic enzyme for NADH is 10-fold lower than for NADPH, the activity reached with the former is significant and this is a remarkable difference respect to other TRXRs, which exhibit a high specificity toward NADPH [20]. Alternatively, the kinetic parameters for disulfide substrates (such as DTNB, *Ec*TRX, *Eh*TRX8 and *Eh*TRX41) were evaluated using both NADPH as NADH as substrates. As shown in Table 2, the substitution of NADPH by NADH did not modify appreciably the kinetic parameters for disulfide substrates. These results support that the enzyme follows a "ping-pong" mechanism, as it was mentioned above. Results support that *Eh*TRXR can use NADPH or NADH as reduced cofactor, being an exception to the rule for specificity of TRXRs for NADPH. In addition, the disulfide reductase activity of *Eh*TRXR was sensible to low concentrations

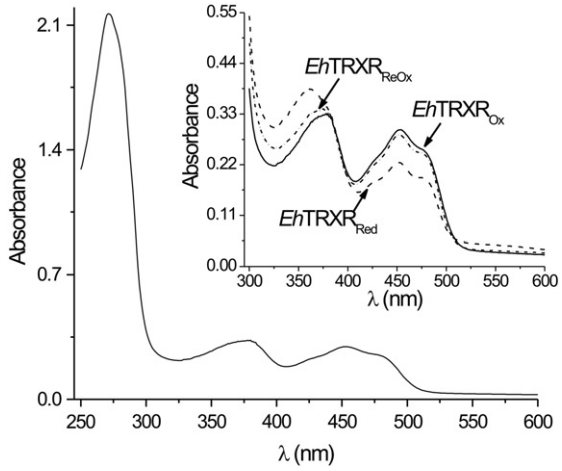

Fig. 1. UV–vis spectrum of purified *Eh*TRXR at 25 °C and pH 7.0. Inset: auto-oxidation of *Eh*TRXR; solid line: untreated *Eh*TRXR, dash line: *Eh*TRXR + 100 μM NADPH and dot-dash line: *Eh*TRXR 1 min after addition of NADPH.

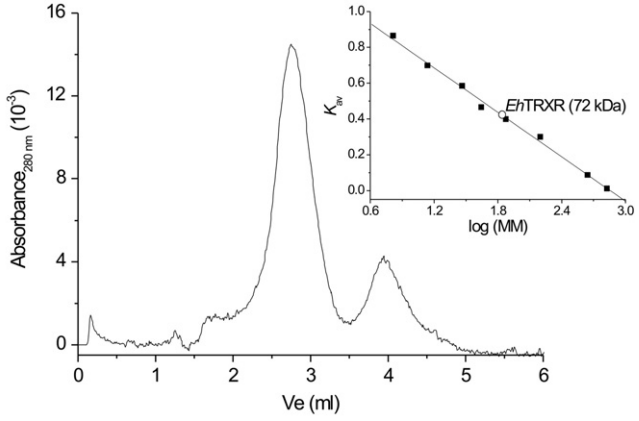

Fig. 3. Gel filtration chromatography of *Eh*TRXR in a Superdex 200 HP Tricorn column. Inset: Plot of K_{av} *vs.* log (molecular mass), (■) standard proteins (○) *Eh*TRXR. All the standard proteins were from GE (Filtration Calibration Kit): Thyroglobulin (669 kDa), Ferritin (440 kDa), Aldolase (158 kDa), Conalbumin (75 kDa), Ovalbumin (43 kDa), Carbonic anhydrase (29 kDa), Ribonuclease A (13.7 kDa) and Aprotinin (6.5 kDa).

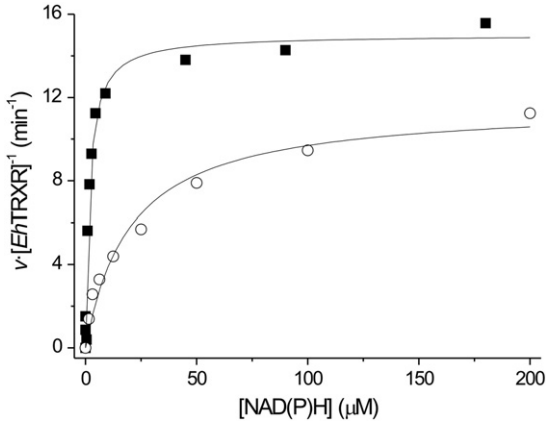

Fig. 4. Kinetic of *Eh*TRXR reduction by NAD(P)H. Assays were performed at 30 °C and pH 7.0 in the presence of 5 mM DTNB and different concentrations of (■) NADPH or (○) NADH.

(<10 μM) of Cu^{2+} and Zn^{2+}. We determined IC_{50} values of 2.5 μM and 3.4 μM for Cu^{2+} and Zn^{2+}, respectively. These results support the participation of cysteine residues in the active site (probably, the CAIC motif) for disulfide reductase activity of this enzyme.

Besides, we evaluated the inhibitory capacity of $NADP^+$ or NAD^+ on the disulfide reductase activity exhibited by *Eh*TRXR using DTNB. NAD^+ acted as poor competitive inhibitor respect to both NADPH and NADH, with K_i values of 1478 μM and 313 μM, respectively. On the other hand, $NADP^+$ performed as a better competitive inhibitor with respect to NADPH or NADH, with K_i values of 26 μM and 7 μM, respectively. These results would indicate that the NADH binding site would be the same as that of NADPH. Union of the latter can be strongly stabilized by the interaction between arginine residues in the binding site of the enzyme the phosphate moiety of NADPH, which explains low K_m value for NADPH and the low K_i value of $NADP^+$ for NADH inhibition. This hypothesis was based on structural descriptions reported for other TRXRs [24]. In addition, no NAD(P)H-dependent reductase activity was detected when the typical substrates (DTNB, and TRXs) were replaced by disulfide glutathione (up to 2 mM), trypanothione disulfide (up to 0.5 mM), lipoamide (up to 2 mM), cystine (up to 2 mM), dehydroascorbic acid (up to 1 mM), selenite (up to 1 mM) or amebic ferredoxins (up to 20 μM) (data non shown). The obtained results agree with previous reports describing few cases of low molecular mass TRXR exhibiting wide substrate specificity [25–27].

3.3. EhTRXR has NAD(P)H dependent H_2O_2-generating oxidase activity

Under aerobic conditions, the purified enzyme showed a NAD(P)H oxidase activity, in the absence of disulfide substrates. We evaluated that *Eh*TRXR produces H_2O_2 by partial reduction of the dissolved O_2 in the reaction mixture. The latter has been verified by means of determination of formed H_2O_2 using the ferrithiocyanide method. The obtained H_2O_2 production rates by means of both NADPH and NADH were comparable, and they exhibited apparent k_{cat} values ~22 min^{-1} (Fig. 5).

Table 1
Kinetic parameters for NAD(P)H oxidation by *Eh*TRXR using 5 mM DTNB as electron acceptor at pH 7.0 and 30 °C.

Coenzyme	K_m (μM)	k_{cat} (min^{-1})	$k_{cat}\cdot K_m^{-1}$ ($M^{-1}\cdot s^{-1}$)
NADPH	1.8	15	1.4×10^5
NADH	23	12	8.4×10^4

Table 2
Kinetic parameters for disulfide reduction by *Eh*TRXR, calculated in the presence of 0.3 mM NADPH or 0.4 mM NADH at pH 7.0 and 30 °C.

Disulfide substrates	NADPH			NADH		
	k_{cat} (min^{-1})	K_m (μM)	$k_{cat}\cdot K_m^{-1}$ ($M^{-1}\cdot s^{-1}$)	k_{cat} (min^{-1})	K_m (μM)	$k_{cat}\cdot K_m^{-1}$ ($M^{-1}\cdot s^{-1}$)
DTNB	15	1100	2.3×10^2	14	1400	1.7×10^2
*Ec*TRX	75	4.7	2.6×10^5	30	6.2	7.5×10^4
*Eh*TRX8	160	2.8	9.5×10^5	155	2.9	8.9×10^5
*Eh*TRX41	130	3.6	6.0×10^5	122	2.3	8.8×10^5

Unlike to disulfide reductase activity, the NAD(P)H oxidase activity of *Eh*TRXR was poorly sensitive to the presence of Cu^{2+} and Zn^{2+} ($IC_{50}>100$ μM). In addition, the pH profiles of disulfide reductase and NAD(P)H oxidase activity showed differences in the calculated apparent pK_a values (Fig. 6). An apparent pK_a value of 7.3 ± 0.1 was obtained for NADPH oxidase activity, whereas a value of 6.4 ± 0.1 was calculated for disulfide reductase activity (with DTNB as disulfide substrate). The latter is similar to the dithiol pK_a value estimated for TRXRs from *Plasmodium falciparum* and *Drosophila melanogaster* [28,29]. These results indicate that, *a priori*, the NAD(P)H oxidase activity does not require the participation of reactive free thiols in the enzyme, and that likely this activity follows an FAD-dependent mechanism.

3.4. S-nitrosothiols reduction by EhTRXR

Considering that *Eh*TRXR was neither able to reduce cystine nor glutathione disulfide, we investigated its capacity to reduce *S*-nitrosothiols, such as CySNO and GSNO. When the reaction mixture containing NADPH and *Eh*TRXR was supplemented with diverse concentrations of both CySNO and GSNO rates of NADPH oxidation were increased proportionally, indicating that these compounds (CySNO or GSNO) can be reduced in a reaction catalyzed by *Eh*TRXR. *S*-nitrosothiol reduction followed Michaelis–Menten kinetics (Fig. 7), and the kinetic parameters calculated for CySNO and GSNO are listed in Table 3. The enzyme exhibited a greater k_{cat} value for the reduction of CySNO compared with GSNO (~6 fold), with similar K_m values for both CySNO and GSNO. Catalytic efficiency ($k_{cat}\cdot K_m^{-1}$) values for GSNO reduction are comparable with kinetic parameters reported for the behavior of other high molecular mass TRXRs (*Plasmodium falciparum*, 10^3 $M^{-1}\cdot s^{-1}$ and calf thymus, 10^5 $M^{-1}\cdot s^{-1}$) [30,31].

In addition, we observed an increase in NADPH oxidation when the reaction was carried out in the presence of *Ec*TRX or *Eh*TRX41, indicating that both *Eh*TRXR and TRX contributed to *S*-nitrosothiol

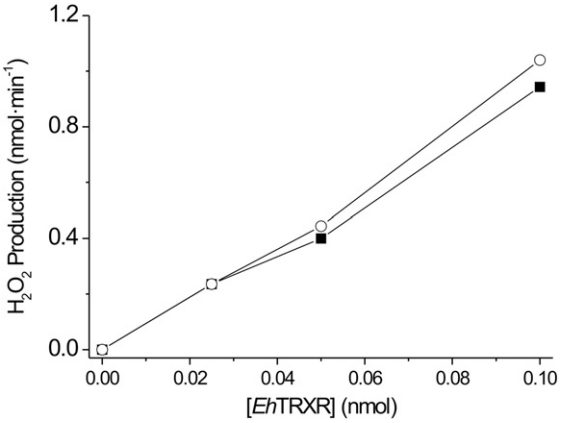

Fig. 5. H_2O_2 production by *Eh*TRXR. The reactions were performed at pH 7.0 and 30 °C in the presence of 300 μM of NADPH (■) or 300 μM of NADH (○) and the specified concentrations of *Eh*TRXR.

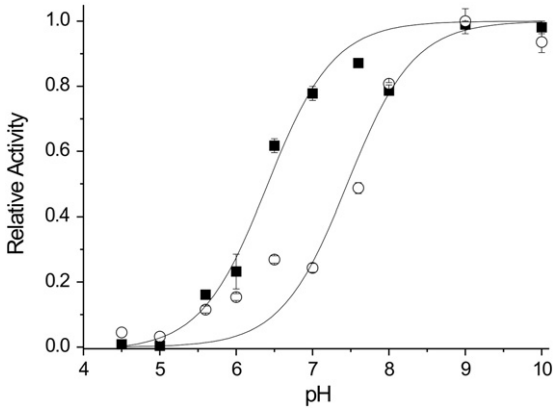

Fig. 6. pH-dependent activity profile of *Eh*TRXR for disulfur reductase (■) or NADPH oxidase (○) activity. Assays were performed at 30 °C in 100 mM potassium phosphate at different pH values. The calculated apparent pK_a values were 6.4 ± 0.1 for disulfure reductase activity and 7.3 ± 0.1 for NADPH oxidase activity. pK_a values are the mean of at least three independent sets of data.

reduction in a synergistic action (catalytic efficiencies values in the presence of *Ec*TRX or *Eh*TRX41 are listed in Table 3). This particular behavior of *Eh*TRXR distinguishes it from other TRXRs that require TRX for *S*-nitrosothiol reduction, as are the cases of the enzymes from *Mycobacterium tuberculosis* or *E. coli* [31,32]. Indeed, our results indicate that *Eh*TRXR has a kinetic performance similar to that of high molecular mass TRXR.

3.5. Quinone reductase activity of EhTRXR

To further study the properties of *Eh*TRXR we sought for the ability of the enzyme to reduce quinones, specifically 2-methyl benzoquinone (MBQ) and 2′-5′di-tert-butyl benzoquinone (DTBBQ). Steady state kinetics indicated that the enzyme performed Michaelis–Menten patterns for quinone reduction, following a hybrid "ping-pong" mechanism. The kinetic parameters for MBQ and DTBBQ are detailed in Table 4. The enzyme showed similar catalytic efficiency for DTBBQ and MBQ reduction, probably due to the high reduction potential presented by both quinones (~210 mV [19]). Furthermore, the presence of MBQ or DTBBQ caused an inhibitory effect on DTNB reduction. MBQ acted as mixed inhibitor respect to DTNB with K_{ic} value of 2.5 μM and K_{iu} value of 3.7 μM. This would indicate that MBQ reduction could also occur via the $FADH_2$ bound to the enzyme, as it was observed for O_2 reduction. Supporting our observations, MBQ reduction was insensible to the presence of Cu^{2+} or Zn^{2+} ($IC_{50} > 200$ μM). Additionally, $NADP^+$ acted as a competitive inhibitor with respect to MBQ ($K_i = 550$ μM). In the case of DTBBQ, the enzyme acted also as a competitive inhibitor with respect to DTNB ($K_i = 105$ μM), being DTBBQ reduction sensible to the presence of Cu^{2+} or Zn^{2+} (IC_{50} ~ 2.6 μM for both heavy metals). These results strongly support that reduction of this substituted quinone by *Eh*TRXR could occur through a mechanism analogous to disulfide substrate reduction. No enzyme inactivation was observed during both quinone reductions, in all cases reaching a stoichiometric oxidation of NADPH with respect to the quinone concentration present in reaction mixture.

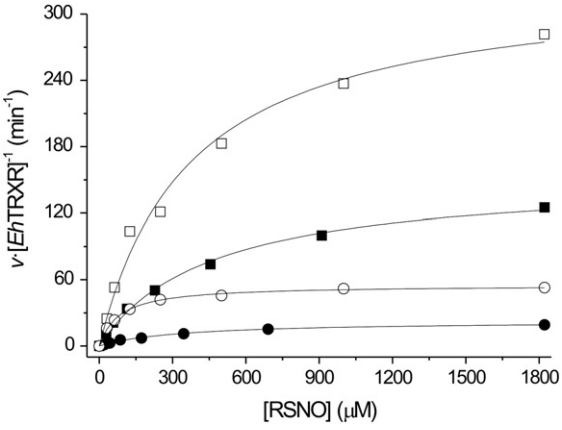

Fig. 7. NADPH-dependent reduction of *S*-nitrosothiols by *Eh*TRXR. Assays were performed at 30 °C and pH 7.0 with 300 μM NADPH, different concentrations of CySNO (squares) or GSNO (circles) in the absence (closed) or in the presence (open) of *Eh*TRX41 5 μM.

Table 3
Kinetic parameters for NADPH-dependent reduction of *S*-nitrosothiols by *Eh*TRXR at pH 7.0 and 30 °C.

S-nitrosothiol	K_m (μM)	k_{cat} (min^{-1})	$k_{cat}\cdot K_m^{-1}$ ($M^{-1}\cdot s^{-1}$)	$k_{cat}\cdot K_m^{-1}$ ($M^{-1}\cdot s^{-1}$) + *Ec*TRX 5 μM	$k_{cat}\cdot K_m^{-1}$ ($M^{-1}\cdot s^{-1}$) + *Eh*TRX41 5 μM
CySNO	452	152	5.6×10^3	1.2×10^3	1.4×10^4
GSNO	342	23	1.1×10^3	1.1×10^4	1.1×10^4

3.6. Diaphorase activity of EhTRXR

We evaluated the diaphorase activity of *Eh*TRXR by means of NADPH-dependent reduction of methylene blue (MB) or potassium ferricyanide [$Fe(CN)_6^{3-}$] or methyl viologen (MV) or 1-chloro-2,4-dinitrobenzene (CDNB), following absorbance decreases at 340 nm. The kinetic data demonstrated that these compounds acted as electron acceptor substrates for the enzyme and their reduction followed Michaelis–Menten kinetics (see Table 4). Thus, the kinetic parameters were similar to those previously reported for other flavoenzymes, such as glutathione reductase from *P. falciparum* and trypanothione reductase from *Trypanosoma brucei* [33,34].

In the case of MB, the catalytic efficiency for its reduction by *Eh*TRXR indicated that this compound is an excellent substrate, since the enzyme catalyzes the spontaneous reaction between NADPH and MB ($k = 3.6\ M^{-1}\cdot s^{-1}$ [34]), by increasing its velocity by five orders of magnitude. MB acted as mixed inhibitor with respect to DTNB in disulfide reductase activity, with a strong competitive component. Calculated inhibition constant values were: $K_{ic} = 3$ μM and $K_{iu} = 106$ μM. These results indicated that the MB reduction would be related to the disulfide reduction mechanism associated to reactive thiols in the enzyme. The latter is consistent with an addition-displacement mechanism, exhibited by thiol-dependent compounds such as glutathione or trypanothione, or dithiol proteins as TRX or tryparedoxin [33]. In support to our findings, $NADP^+$ acted as mixed inhibitor respect to MB ($K_{ic} = 2.8$ mM and $K_{iu} = 6$ mM).

3.7. EhTRXR reduction potential determination

In agreement to Haldane relationships, the ratio between the direct to inverse bimolecular rate constants gives the apparent equilibrium

Table 4
Kinetic parameters for non-disulfide substrates reduction by *Eh*TRXR in the presence of 0.3 mM NADPH at pH 7.0 and 30 °C.

Compound	K_m (μM)	k_{cat} (min^{-1})	$k_{cat}\cdot K_m^{-1}$ ($M^{-1}\cdot s^{-1}$)
MBQ	92	568	1.0×10^5
DTBBQ	7	57	1.4×10^5
MB	20	210	1.7×10^5
$Fe(CN)_6^{3-}$	293	370	2.1×10^4
MV	184	161	1.4×10^4
CDNB	105	298	4.7×10^4

constant ($K_{eq\ app}$) of the catalyzed reaction. For the reductive semireaction: NADPH + *Eh*TRXR$_{Ox}$ ↔ NADP$^+$ + *Eh*TRXR$_{Red}$, the $K_{eq\ app}$ can be calculated as the ratio of $k_{cat}\cdot K_m^{-1}$ for direct reaction respect to $k_{cat}\cdot K_m^{-1}$ of the inverse reaction. In addition, for the oxidative semireaction: *Ec*TRX$_{Ox}$ + *Eh*TRXR$_{Red}$ ↔ *Ec*TRX$_{Red}$ + *Eh*TRXR$_{Ox}$, the $K_{eq\ app}$ can be calculated in similar form as a ratio of $k_{cat}\cdot K_m^{-1}$ for each reaction sense. Our results support that the TRX reduction reaction is reversible since *Eh*TRXR effectively catalyzed both directions of the reaction. Also, similar K_m values for *Ec*TRX were obtained in both directions of the reaction, which would indicate, that the binding of these proteins are not influenced by their individual redox states. From each $k_{cat}\cdot K_m^{-1}$ ratio we calculated the $K_{eq\ app}$ for the respective semireaction and, utilizing the Nernst equation, we obtained the global $E^{o\prime}$ for *Eh*TRXR (Table 5). Values of $E^{o\prime}$ for *Eh*TRXR derived from both reductive and oxidative semireaction are similar, averaging in −292 mV.

3.8. Resistance to oxidative damage

We utilized the disk inhibition assay to test whether *Eh*TRXR would protect against oxidative damage in bacteria cells. As shown in Fig. 8, inhibition rings were observed either in the presence of 20 or 200 mM diamide. We found that *Eh*TRXR-transformed *E. coli* cells underwent less growth arrest than the control (pET28 transformed *E. coli* cells), indicating that *Eh*TRXR-overexpressing cells were to some extent more tolerant to diamide-mediated oxidative damage. No difference between recombinant bacteria cell growth under non-stress condition was observed (data not shown).

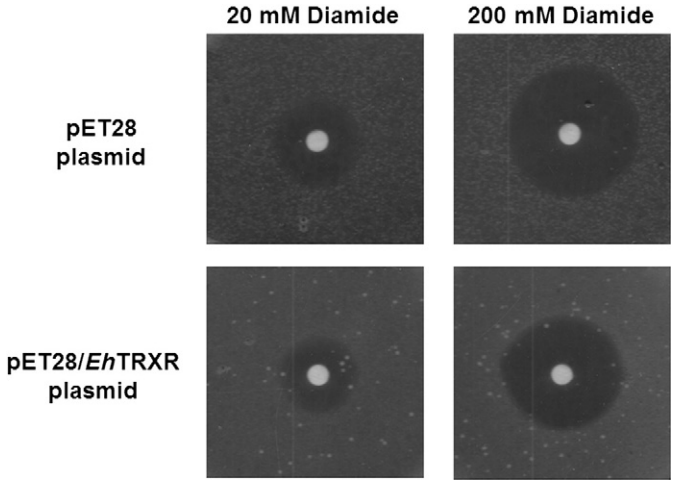

Fig. 8. Effect of diamide on disk inhibition assays for growing of transformed *E. coli*. The top panel shows *E. coli* cells transformed with the pET28 vector. The bottom panel corresponds to *E. coli* cells transformed with the pET 28/*Eh*TRXR vector. The differences between control and *Eh*TRXR transformed cells were reliable after repetition in three independent experiences.

4. Discussion and conclusions

The enteric unicellular parasite *E. histolytica* is the causative agent of amoebiasis, a disease that is surpassed only by malaria as a parasitic cause of death [2]. Normally resident of the large bowel, *E. histolytica* occasionally penetrates the intestinal mucosa and disseminates to other organs [1]. A critical virulence factor of the microorganism is determined by its ability to cope with conditions of increasing oxygen pressures and high ROS and RNS concentrations [2]. We have recently demonstrated the occurrence of TRX systems in *E. histolytica* [11,12], which functionally expands the understanding about redox metabolism in this parasite.

The redox metabolic scenario operating in *E. histolytica* includes the involvement of *Eh*TRXR and *Eh*TRXs as critical in maintaining a redox balance in the parasite cytosol [11,12], being the reductase a relevant enzyme for the viability of the parasite as previously reported by Leitsch et al. and Debnath et al. [35,36]. Herein we further explored catalytic capacity and functional operation of the TRX system in *E. histolytica* to gain a more complete picture about the actual relevance it plays for the parasite coping with different physiological and stress conditions. *Eh*TRXR showed an amino acid sequence highly conserved when compared with those previously reported from other members of the low molecular mass TRXR family [12]. The purified protein exhibited an absorption spectrum characteristic for flavoproteins, having one FAD molecule bound (non-covalently) per enzyme subunit (a structural characteristics conserved also in TRXR from other sources [25]). Non-reducing SDS-PAGE and gel filtration chromatography revealed that *Eh*TRXR presented a native covalent homodimeric structure. Cysteine residues forming the disulfide bridge between subunits seem to be others than those involved in the catalytic function (no change in electrophoretic profiles was observed for the enzyme incubated with NADPH). On the other hand, the complete reduction of all disulfide bridges was observed only when *Eh*TRXR was incubated in the presence of DTT (nonspecific reductant). In a previous work, Alkhalfioui et al. [24] report that TRXR from the leguminous *Medicago truncatula* present cross-linked subunits, the authors attributing such structural characteristic to a C-terminal cysteine. It is tempting to speculate that Cys^{301} in *Eh*TRXR would be playing a similar function. Steady state kinetics indicated that the disulfide reduction catalyzed by *Eh*TRXR followed a "hybrid ping-pong" mechanism with saturation kinetic for both substrates. This means that NAD(P)H and disulfide substrates interact in different active sites, a fact also observed in other pyridine nucleotide disulfide reductases like glutathione reductase or trypanothione reductase [19,33,37]. Additionally, we found that the disulfide reductase activity was sensible to the inhibition by heavy metals, verifying the participation of reactive thiols in the enzyme at least during disulfide substrate reduction as for the case of DTNB.

As above indicated, *Eh*TRXR can utilize either NADPH or NADH as reducing equivalent donors for the disulfide reductase activity. Even when the affinity of the enzyme for NADPH was 10-fold higher than for NADH, the activity exhibited with NADH is noteworthy, especially if compared with TRXRs exhibiting a preference toward NADPH over NADH between two and three orders of magnitude [20,24,38]. The coenzyme binding motif GXGXXG/A is common to many NAD(P)H-dependent enzymes, being decisive for the specificity toward NADH or NADPH the presence in the coenzyme binding domain of acidic (Glu or Asp) or basic (Arg and Lys) residues, respectively [24,39]. Thus, the presence of acidic residues determines specificity for NADH since the presence of negative charges produces an electrostatic repulsion to the negatively charged phosphate moiety of NADPH (for example, in AhpF enzyme) [39]. On the other hand, the presence of basic residues enhances affinity for NADPH, since these

Table 5
Determination of the macroscopic *Eh*TRXR redox potential. The reported values are average of four independent experiments realized at pH 7.0 and 30 °C.

Reductive semireaction			
NADPH + EhTRXR$_{Ox}$ ↔ NADP$^+$ + EhTRXR$_{Red}$			
$k_{cat}\cdot K_m^{-1}$ NADPH ($\mu M^{-1}\ min^{-1}$)	$k_{cat}\cdot K_m^{-1}$ NADP$^+$ ($\mu M^{-1}\ min^{-1}$)	K_{eq}^{app}	$E^{o\prime}_{EhTRXR}$ (mV)
9.5	1.0	9.6	−290 ± 2
Oxidative semireaction			
Ec*TRX$_{Ox}$* + *EhTRXR$_{Red}$* ↔ Ec*TRX$_{Red}$* + *EhTRXR$_{Ox}$*			
$k_{cat}\cdot K_m^{-1}$ *Ec*TRX$_{Ox}$ ($\mu M^{-1}\ min^{-1}$)	$k_{cat}\cdot K_m^{-1}$ *Ec*TRX$_{Red}$ ($\mu M^{-1}\ min^{-1}$)	K_{eq}^{app}	$E^{o\prime}_{EhTRXR}$ (mV)
17.7	7.1	2.5	−295 ± 1

residues favor electrostatic interactions with the phosphate group of NADPH [39]. Nevertheless, the presence of basic residues in the binding domain would not exclude the possibility of using NADH as a reducer substrate. Almost all TRXRs can use NADH as a substrate but with very low affinity (mM concentrations) [20]. There are only a few cases of TRXRs using NADH with comparable efficiencies respect to NADPH [24].

*Eh*TRXR present a coenzyme binding motif (GGGGDAA) conserved in several TRXRs, as well as the presence of residues Arg^{183} and Arg^{184} putatively involved in the interaction with the phosphate moiety of NADPH. Our results indicate that *Eh*TRXR would not strictly follow the rule for NADPH (or NADH) specificity. We wonder about possible physiological advantages in using NADPH and NADH as reducing substrates by *Eh*TRXR. Perhaps, the use of both coenzymes could be a consequence of the intrinsic metabolism of the parasite. This organism lacks an active Krebs cycle with the glycolytic pathway as the primary energy/reduction equivalents producer [1,40]. The latter generates NADH as reduced coenzyme, which could act as electron donor for the catalyzed-transhydrogenation of $NADP^+$ [41]. Another possible NAD(P)H regeneration way would be the dehydrogenase-catalyzed alcohols and aldehydes oxidation [42]. Studies performed on cultures of *E. histolytica* have demonstrated that alcohol dehydrogenase 2 is essential for the survival of this parasite [43]. These mechanisms, for NADPH regeneration, would be important if we consider that the parasite has an incomplete pentose phosphate pathway, lacking the $NADP^+$-dependent enzymes that catalyze the oxidative decarboxylation of Glc-6P to Rib-5P [1]. Consequently, the capacity of *Eh*TRXR to use both NADPH and NADH as electron donors could increase its reduction power capacity obtained under oxidative stress.

The amoebic reductase also exhibited a H_2O_2-generating NAD(P)H oxidase activity in the presence of O_2, following a mechanism found to be different to that corresponding to the disulfide reduction. This was verified by inhibition assays with heavy metals, where the NAD(P)H oxidase activity was 100-fold less sensitive respect to the disulfide reductase activity. Our findings agree with previous reports about other flavoenzymes (including disulfide reductases and oxidases), where the O_2 reduction takes place by direct reaction with $FADH_2$ (prostetic group in reduced form) without intervention of reactive thiols in the enzyme [19]. Physiologically, in *E. histolytica* the oxidase activity would act as a first stage in the O_2 elimination route leading its partial reduction to H_2O_2, thus generating reactive species. It would follow neutralization of the latter compounds by reduction to H_2O toward antioxidant systems (for example, *Eh*2CysPrx or cysteine) to avoid cellular damages [11,12]. Similar processes have been described in other protozoa like *T. vaginalis* [44].

In the present work we evidence the capacity of *Eh*TRXR to catalyze direct NADPH-dependent reduction of GSNO and CySNO. The enzyme exhibited no significant difference respect to its affinity by these compounds, but presenting lower (~7-fold) activity with GSNO than with CySNO. These differences in reactivity could be due to enzyme specificity for CySNO as part of an antioxidant system against the stress generated by reactive nitrogen species. Even when K_m values for CysNO and GSNO are rather elevated, it is worth to consider the high k_{cat} exhibited by the enzyme, which result that catalytic efficiency ($k_{cat} \cdot K_m^{-1}$) are comparable with other TRXRs found to play a physiological function in different cells [30,31]. Because of the low levels of glutathione (and consequently those of GSNO) found in *E. histolytica*, the formation of *S*-nitrosothiols in the parasite would depend on intracellular cysteine. Possibly, the cysteinyl radical species (thiyl radicals) present in the parasite would react with exogenous NO (or derived-species) generating CySNO [45]. A similar mechanism for GSNO detoxification has been previously described in *P. falciparum* and mammals [30,31]. Additionally, the increased catalytic efficiency for *S*-nitrosothiols reduction observed in the presence of TRX support a synergistic action involving both proteins. Overall, our results support the idea that *Eh*TRXR and *Eh*TRXs could represent an important mechanism to regulate intracellular levels of CySNO in *E. histolytica* living under oxidative or nitrosative stress conditions.

The capacity of *Eh*TRXR to catalyze the reversible transference of reduction equivalents from NADPH to oxidized TRX was utilized to determine the reduction potential of the enzyme (−292 mV). This value is in agreement with those reported for TRXRs from rat and *Drosophila melanogaster*; −294 mV and −293 mV respectively [19,20]. There is a thermodynamic coherence between the calculated reduction potential of *Eh*TRXR, the corresponding potential to NAD(P)H (−320 mV), and *Eh*TRXs (−283 mV) [11], which is indicative of the potential physiological operation of the system for reduction equivalents transference in the parasite. Conclusively, the presence of *Eh*TRXR and *Eh*TRXs coupled to *Eh*2CysPrx would be associated to an antioxidant functional system in *E. histolytica*, as summarized in Fig. 9.

In the present work it is also evidenced that *Eh*TRXR can use non-physiological substrates, such as quinones and redox dyes, exhibiting similar catalytic efficiency to that showed for TRX. Inhibition profiles of diaphorase (by $NADP^+$) and disulfide reductase activity (by non-physiological substrates) indicate that the reduction mechanism of non-physiological substrates can involve both thiol-dependent and flavine-dependent pathways. Kinetic parameters obtained for quinone reduction agree with those reported for TRXR from mammal and *Arabidopsis thaliana* [19,23]. On the other hand, the observed competitive inhibition of MB in disulfide reductase

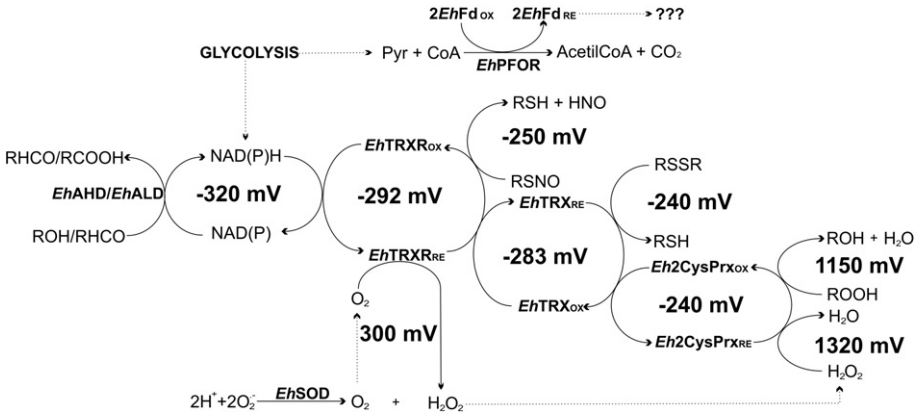

Fig. 9. Schematic representation of thioredoxin system in *Entamoeba histolytica* associated with other previously characterized systems. *Eh*AHD: alcohol dehydrogenase; *Eh*ALD: aldehyde dehydrogenase; *Eh*Fd: ferredoxin; *Eh*PFOR: pyruvate ferredoxin oxidoreductase; *Eh*SOD: superoxide dismutase; *Eh*TRXR: thioredoxin reductase; *Eh*TRX: thioredoxin; *Eh*2CysPrx: 2Cys peroxiredoxin; RSH: low molecular mass thiol; RSSR: low molecular mass disulfide; RSNO *S*-nitrosothiol, ROOH; organic hydroperoxide; RHCO: aldehyde; ROH: alcohol; RCOOH: organic acid.

activity of *Eh*TRXR does not correlate with results obtained by others for human and *P. falciparum* glutathione reductases, for *T. brucei* trypanothione reductase, or for *P. falciparum* TRXR, where MB was characterized as a noncompetitive inhibitor [33,34]. The authors described the existence of direct electron transference between $FADH_2$ and MB without intervention of reactive cysteine residues of the involved enzymes. However, the possibility that *Eh*TRXR can reduce MB via $FADH_2$ should not be discarded. The non-physiological substrates exhibited an efficient inhibitory effect on disulfide reductase activity of the *E. histolytica* enzyme, presenting low values of K_i. Particularly, MB demonstrated to act as a subversive substrate, since it was not only able to take the reducing equivalent from the enzyme, but acted as an oxidative species generator when oxidized in the presence of O_2, creating a futile redox cycle [33]. The present work improves the knowledge about kinetic, structural and thermodynamic properties of *Eh*TRXR, which reinforces the functionality of the TRX system as a central node for the redox equivalents flux in *E. histolytica*. As schematized in Fig. 9, the TRX system in this parasite appears as an important cellular tool for the parasite defense against damaging oxidative species derived from oxygen and nitrogen during the extraintestinal phase of the amoebic infection.

Acknowledgments

This work was supported by grants from UNL (CAI + D Orientados & Redes), CONICET (PIP 112 2008-01-02519 and PIP 114 2011-01-00168) and ANPCyT (PICT'07 668, PICT'08 1754). DGA, AAI and SAG are investigator career members from CONICET.

References

[1] B. Loftus, I. Anderson, R. Davies, U.C. Alsmark, J. Samuelson, P. Amedeo, P. Roncaglia, M. Berriman, R.P. Hirt, B.J. Mann, T. Nozaki, B. Suh, M. Pop, M. Duchene, J. Ackers, E. Tannich, M. Leippe, M. Hofer, I. Bruchhaus, U. Willhoeft, A. Bhattacharya, T. Chillingworth, C. Churcher, Z. Hance, B. Harris, D. Harris, K. Jagels, S. Moule, K. Mungall, D. Ormond, R. Squares, S. Whitehead, M.A. Quail, E. Rabbinowitsch, H. Norbertczak, C. Price, Z. Wang, N. Guillen, C. Gilchrist, S.E. Stroup, S. Bhattacharya, A. Lohia, P.G. Foster, T. Sicheritz-Ponten, C. Weber, U. Singh, C. Mukherjee, N.M. El-Sayed, W.A. Petri Jr., C.G. Clark, T.M. Embley, B. Barrell, C.M. Fraser, N. Hall, The genome of the protist parasite *Entamoeba histolytica*, Nature 433 (2005) 865–868.
[2] M.A. Akbar, N.S. Chatterjee, P. Sen, A. Debnath, A. Pal, T. Bera, P. Das, Genes induced by a high-oxygen environment in *Entamoeba histolytica*, Mol. Biochem. Parasitol. 133 (2004) 187–196.
[3] I.J. Anderson, B.J. Loftus, *Entamoeba histolytica*: observations on metabolism based on the genome sequence, Exp. Parasitol. 110 (2005) 173–177.
[4] E. Ramos-Martinez, A. Olivos-Garcia, E. Saavedra, M. Nequiz, E.C. Sanchez, E. Tello, M. El-Hafidi, A. Saralegui, E. Pineda, J. Delgado, I. Montfort, R. Perez-Tamayosb: authors>*Entamoeba histolytica*: oxygen resistance and virulence Int. J. Parasitol. 39 (2009) 693–702.
[5] M.R. Ariyanayagam, A.H. Fairlamb, *Entamoeba histolytica* lacks trypanothione metabolism, Mol. Biochem. Parasitol. 103 (1999) 61–69.
[6] H. Al-Sa'doni, A. Ferro, S-Nitrosothiols: a class of nitric oxide-donor drugs, Clin. Sci. (Lond.) 98 (2000) 507–520.
[7] R. Siman-Tov, S. Ankri, Nitric oxide inhibits cysteine proteinases and alcohol dehydrogenase 2 of *Entamoeba histolytica*, Parasitol. Res. 89 (2003) 146–149.
[8] B. Halliwell, Reactive species and antioxidants. Redox biology is a fundamental theme of aerobic life, Plant Physiol. 141 (2006) 312–322.
[9] A. Holmgren, C. Johansson, C. Berndt, M.E. Lonn, C. Hudemann, C.H. Lillig, Thiol redox control via thioredoxin and glutaredoxin systems, Biochem. Soc. Trans. 33 (2005) 1375–1377.
[10] T. Jaeger, L. Flohe, The thiol-based redox networks of pathogens: unexploited targets in the search for new drugs, Biofactors 27 (2006) 109–120.
[11] D.G. Arias, P.G. Carranza, H.D. Lujan, A.A. Iglesias, S.A. Guerrero, Immunolocalization and enzymatic functional characterization of the thioredoxin system in *Entamoeba histolytica*, Free Radic. Biol. Med. 45 (2008) 32–39.
[12] D.G. Arias, C.E. Gutierrez, A.A. Iglesias, S.A. Guerrero, Thioredoxin-linked metabolism in *Entamoeba histolytica*, Free Radic. Biol. Med. 42 (2007) 1496–1505.
[13] U.K. Laemmli, Cleavage of structural proteins during the assembly of the head of bacteriophage T4, Nature 227 (1970) 680–685.
[14] K.A. Ferguson, Starch-gel electrophoresis—application to the classification of pituitary proteins and polypeptides, Metabolism 13 (1964) 985–1002 (Suppl.).
[15] M.M. Bradford, A rapid and sensitive method for the quantitation of microgram quantities of protein utilizing the principle of protein-dye binding, Anal. Biochem. 72 (1976) 248–254.
[16] M.P. Gordge, J.S. Hothersall, A.A. Noronha-Dutra, Evidence for a cyclic GMP-independent mechanism in the anti-platelet action of S-nitrosoglutathione, Br. J. Pharmacol. 124 (1998) 141–148.
[17] P. Eyer, F. Worek, D. Kiderlen, G. Sinko, A. Stuglin, V. Simeon-Rudolf, E. Reiner, Molar absorption coefficients for the reduced Ellman reagent: reassessment, Anal. Biochem. 312 (2003) 224–227.
[18] R. Chauhan, S.C. Mande, Characterization of the *Mycobacterium tuberculosis* H37Rv alkyl hydroperoxidase AhpC points to the importance of ionic interactions in oligomerization and activity, Biochem. J. 354 (2001) 209–215.
[19] N. Cenas, H. Nivinskas, Z. Anusevicius, J. Sarlauskas, F. Lederer, E.S. Arner, Interactions of quinones with thioredoxin reductase: a challenge to the antioxidant role of the mammalian selenoprotein, J. Biol. Chem. 279 (2004) 2583–2592.
[20] Z. Cheng, L.D. Arscott, D.P. Ballou, C.H. Williams Jr., The relationship of the redox potentials of thioredoxin and thioredoxin reductase from *Drosophila melanogaster* to the enzymatic mechanism: reduced thioredoxin is the reductant of glutathione in *Drosophila*, Biochemistry 46 (2007) 7875–7885.
[21] R.A. Alberty, Relations between biochemical thermodynamics and biochemical kinetics, Biophys. Chem. 124 (2006) 11–17.
[22] D. Mustacich, G. Powis, Thioredoxin reductase, Biochem. J. 346 (Pt 1) (2000) 1–8.
[23] D. Bironaite, Z. Anusevicius, J.P. Jacquot, N. Cenas, Interaction of quinones with *Arabidopsis thaliana* thioredoxin reductase, Biochim. Biophys. Acta 1383 (1998) 82–92.
[24] F. Alkhalfioui, M. Renard, F. Montrichard, Unique properties of NADP-thioredoxin reductase C in legumes, J. Exp. Bot. 58 (2007) 969–978.
[25] A. Holmgren, M. Bjornstedt, Thioredoxin and thioredoxin reductase, Methods Enzymol. 252 (1995) 199–208.
[26] T. Tamura, T.C. Stadtman, Mammalian thioredoxin reductases, Methods Enzymol. 347 (2002) 297–306.
[27] E.S. Arner, L. Zhong, A. Holmgren, Preparation and assay of mammalian thioredoxin and thioredoxin reductase, Methods Enzymol. 300 (1999) 226–239.
[28] P.J. McMillan, L.D. Arscott, D.P. Ballou, K. Becker, C.H. Williams Jr., S. Muller, Identification of acid–base catalytic residues of high-Mr thioredoxin reductase from *Plasmodium falciparum*, J. Biol. Chem. 281 (2006) 32967–32977.
[29] H.H. Huang, L.D. Arscott, D.P. Ballou, C.H. Williams Jr., Acid–base catalysis in the mechanism of thioredoxin reductase from *Drosophila melanogaster*, Biochemistry 47 (2008) 1721–1731.
[30] S.M. Kanzok, S. Rahlfs, K. Becker, R.H. Schirmer, Thioredoxin, thioredoxin reductase, and thioredoxin peroxidase of malaria parasite *Plasmodium falciparum*, Methods Enzymol. 347 (2002) 370–381.
[31] D. Nikitovic, A. Holmgren, S-nitrosoglutathione is cleaved by the thioredoxin system with liberation of glutathione and redox regulating nitric oxide, J. Biol. Chem. 271 (1996) 19180–19185.
[32] R. Attarian, C. Bennie, H. Bach, Y. Av-Gay, Glutathione disulfide and S-nitrosoglutathione detoxification by *Mycobacterium tuberculosis* thioredoxin system, FEBS Lett. 583 (2009) 3215–3220.
[33] K. Buchholz, M.A. Comini, D. Wissenbach, R.H. Schirmer, R.L. Krauth-Siegel, S. Gromer, Cytotoxic interactions of methylene blue with trypanosomatid-specific disulfide reductases and their dithiol products, Mol. Biochem. Parasitol. 160 (2008) 65–69.
[34] K. Buchholz, R.H. Schirmer, J.K. Eubel, M.B. Akoachere, T. Dandekar, K. Becker, S. Gromer, Interactions of methylene blue with human disulfide reductases and their orthologues from *Plasmodium falciparum*, Antimicrob. Agents Chemother. 52 (2008) 183–191.
[35] D. Leitsch, D. Kolarich, I.B. Wilson, F. Altmann, M. Duchene, Nitroimidazole action in *Entamoeba histolytica*: a central role for thioredoxin reductase, PLoS Biol. 5 (2007) e211.
[36] A. Debnath, D. Parsonage, R.M. Andrade, C. He, E.R. Cobo, K. Hirata, S. Chen, G. Garcia-Rivera, E. Orozco, M.B. Martinez, S.S. Gunatilleke, A.M. Barrios, M.R. Arkin, L.B. Poole, J.H. McKerrow, S.L. Reed, A high-throughput drug screen for Entamoeba histolytica identifies a new lead and target, Nat. Med. 18 (2012) 956–960.
[37] D.G. Arias, V.E. Marquez, A.J. Beccaria, S.A. Guerrero, A.A. Iglesias, Purification and characterization of a glutathione reductase from Phaeodactylum tricornutum, Protist 161 (2010) 91–101.
[38] A.J. Serrato, J.M. Perez-Ruiz, F.J. Cejudo, Cloning of thioredoxin h reductase and characterization of the thioredoxin reductase-thioredoxin h system from wheat, Biochem. J. 367 (2002) 491–497.
[39] C.M. Reynolds, J. Meyer, L.B. Poole, An NADH-dependent bacterial thioredoxin reductase-like protein in conjunction with a glutaredoxin homologue form a unique peroxiredoxin (AhpC) reducing system in *Clostridium pasteurianum*, Biochemistry 41 (2002) 1990–2001.
[40] J. McLaughlin, S. Aley, The biochemistry and functional morphology of the Entamoeba, J. Protozool. 32 (1985) 221–240.
[41] C.J. Weston, S.A. White, J.B. Jackson, The unusual transhydrogenase of *Entamoeba histolytica*, FEBS Lett. 488 (2001) 51–54.
[42] A. Kumar, P.S. Shen, S. Descoteaux, J. Pohl, G. Bailey, J. Samuelson, Cloning and expression of an NADP(+)-dependent alcohol dehydrogenase gene of *Entamoeba histolytica*, Proc. Natl. Acad. Sci. U. S. A. 89 (1992) 10188–10192.
[43] A. Espinosa, D. Clark, S.L. Stanley Jr., *Entamoeba histolytica* alcohol dehydrogenase 2 (EhADH2) as a target for anti-amoebic agents, J. Antimicrob. Chemother. 54 (2004) 56–59.
[44] G.H. Coombs, G.D. Westrop, P. Suchan, G. Puzova, R.P. Hirt, T.M. Embley, J.C. Mottram, S. Muller, The amitochondriate eukaryote *Trichomonas vaginalis* contains a divergent thioredoxin-linked peroxiredoxin antioxidant system, J. Biol. Chem. 279 (2004) 5249–5256.
[45] K.A. Broniowska, N. Hogg, The Chemical Biology of S-Nitrosothiols, Antioxid. Redox. Signal. 17 (2012) 969–980.